International Journal on Recent and Innovation Trends in Computing and Communication
ISSN: 2321-8169 Volume: 11 Issue: 9
***Article Received:** 25 July 2023 **Revised:** 12 September 2023 **Accepted:** 30 September 2023*

The Effect of Crop Growth Stage on the Formation And Ability of Carbon Occlusion within Phytoliths in Rice Varieties

R. Vidhya1, L. Arul Pragasan2*
1Research Scholar, Environmental Ecology Laboratory, Department of Environmental Sciences, Bharathiar University, Coimbatore, Tamil Nadu -641046, India.
2*Assistant Professor, Environmental Ecology Laboratory, Department of Environmental Sciences, Bharathiar University, Coimbatore, Tamil Nadu -641046, India.
2*Corresponding author E-mail: arulpragasan0504@gmail.com

Abstract- Carbon occlusion refers to the process by which carbon dioxide is incorporated into the silica structure of phytoliths during their formation. Microscopic silica formations called phytoliths develop inside plant cells. Phytoliths are microscopic, silica-based structures that develop inside plant cells. These silica bodies are deposited in various parts of the plant, such as leaves, stems, and reproductive organs. Carbon occlusion within phytoliths can potentially act as a long-term carbon sink, aiding in the mitigation of greenhouse gas emissions and climate change. They are commonly found in various plant species, including rice. This study focuses on investigating how the growth stage of rice crops affects the process of carbon occlusion within phytoliths. Phytoliths play important roles in plant structure, defense mechanisms, and carbon storage. The research study aims to examine how different growth stages of rice crops influence the formation of phytoliths and the extent to which carbon is occluded within them. It may involve conducting experiments or observations at different growth stages of rice plants, such as the seedling stage, vegetative stage, flowering stage, or maturity stage. The findings of this research could contribute to our understanding of the carbon sequestration potential of rice crops and how it varies throughout their growth cycle.
Keywords: carbon occlusion; phytolith organic carbon; below-ground biomass; above-ground biomass; phytolith morphotypes.

1. INTRODUCTION

Rice (Oryza sativa) is not only a staple food for a significant portion of the world's population but also a crucial crop in global agricultural systems [1]. As the global population continues to grow, the need for sustainable rice production becomes increasingly urgent [2]. Examining agricultural methods that aid in carbon sequestration and greenhouse gas emissions reduction has recently attracted more attention [3][4]. Among the potential strategies, the role of phytoliths, silica bodies formed within plants, has garnered attention due to their capacity for carbon occlusion and long-term carbon storage in agroecosystems. Phytoliths are produced through biomineralization processes, where silica is taken up from the surrounding environment and deposited as silica dioxide (SiO2) within plant cells [5]. Besides their structural functions, such as providing support and defense against herbivores and pathogens, phytoliths have emerged as an intriguing component in the carbon cycle [6][7].

Recent research suggests that phytoliths can act as a carbon sink by occluding carbon dioxide during their formation [8][9]. This process, known as carbon occlusion, has the potential to contribute significantly to carbon sequestration in agricultural systems [10]. Several factors influence the formation and carbon occlusion capacity of phytoliths, including plant species, environmental conditions, and developmental stages. In the context of rice production, understanding the effect of the crop growth stage on phytolith formation and carbon occlusion becomes particularly relevant. Different growth stages in rice plants exhibit distinct physiological characteristics, such as leaf development, root system establishment, and grain filling [11][12][13]. These variations can potentially influence the quantity and quality of phytoliths formed, ultimately impacting their carbon occlusion capacity. Investigating the relationship between crop growth stage and the formation and ability of carbon occlusion within phytoliths is essential for optimizing carbon sequestration strategies in rice production systems. By identifying the growth stages that offer the greatest potential for enhancing carbon storage, researchers can develop targeted approaches to maximize carbon sequestration in rice crops.

This study aims to examine the influence of the crop growth stage on the formation and ability of carbon occlusion within phytoliths in different rice varieties. By analyzing the phytolith content and carbon occlusion capacity at various growth stages, we seek to identify the optimal stage for promoting carbon sequestration in rice plants. Additionally, we will assess potential variability in phytolith characteristics and carbon occlusion capacity among different rice varieties,

International Journal on Recent and Innovation Trends in Computing and Communication
ISSN: 2321-8169 Volume: 11 Issue: 9
***Article Received:** 25 July 2023 **Revised:** 12 September 2023 **Accepted:** 30 September 2023*

considering their implications for crop management and breeding programs focused on improving carbon sequestration efficiency [14][15]. The paper is organized as follows: The review of the paper is covered in Section 2, the materials and models for the rice variety are covered in Section 3, the results of the Phytolith Concentration, Carbon Concentration, Phytolith Concentration, Phytolith Flux Production, and Phytolith Production Rate are covered in Section 4, and the discussion of Phytolith and its Morphotypes is covered in Section 5, and the paper is concluded in Section 6.

2. LITERATURE REVIEW

Sun et al. 2016 [16] evaluated the carbon bio-sequestration within the phytoliths generated in the rice seed husks of 35 different rice cultivars to pinpoint rice cultivars with comparatively higher phytolith carbon sequestration efficiency.

Zuo et al. 2014 [17] looked at how soil PhytOC was distributed in the Chinese Loess Plateau (CLP). Higher plants produce minute particles called phytoliths, also known as silica(si) bodies, which accumulate inside their cells and cell walls.

Ru et al. 2018 [18] studied the formation of phytoliths and PhytOC, as well as the contents of phytoliths and PhytOC, in sandy grassland with varied vegetation covering in eastern Inner Mongolia, China.

Yang et al. 2015 [19] calculated the production of PhytOC in the forests of northern China by measuring the Silica levels of 108 plant species from Inner Mongolia and Hebei, China, to demonstrate the relationships between plant Si content and other phylogenetic and ecological features.

Yang et al. 2020 [20] evaluated the long-term effects on labile Si fractions in paddy soil and subsequent plant Si uptake of groundwater table control and phytolith-rich straw return. Si et al. 2018 [21] showed that the presence of Si in the medium had an impact on the uptake of lanthanum (La) by rice seedlings, and that phytolith was essential for the bio-sequestration of La and for mitigating the harm that La caused to rice seedlings.

Anjum and Nagabovanalli 2021 [22] collected ground-level biomass samples from 22 ecosystems of highly farmed rice to assess the rate of carbon sequestration by phytoliths. A significant source of long-term C storage in agroecosystems is the carbon that is stable and occluded in phytoliths. As a crop that accumulates silicon (Si), rice produces a lot of PhytOC, which is essential for the coupled C and Si biogeochemical cycle.

Wang et al. 2019 [23] assessed the long-term impacts of tillage strategies on aggregate-associated carbon (C), aggregate-associated water-stable aggregates, and C storage in a double rice production system in southern China. climate change mitigation. Farmland soil conservation, nutrient supply potential, and are all significantly influenced by soil structural stability and carbon (C) storage.

Weisskopf et al. 2014 [24] concentrated on analyzing archaeobotanical assemblages using contemporary analog phytolith assemblages of companion crop weeds seen in cultivation regimes as well as in wild rice stands.

3. PROPOSED METHODOLOGIES

A. Materials and Methods

1. Collection of Rice Crops

The study region consists of the dominating rice-growing areas in Tamil Nadu. Samples of 1009 and CO 51 rice varieties were collected from Thanjavur and 50/16, ponmani, and thuyamalli from Nagercoil. Figure 1 shows the study region where the rice varieties were collected. Three replicates of each of the five rice kinds were randomly selected at different growth phases, i.e., first stage = 40th day, second stage = 80th day, and third stage = 120th day. This crop sample was carefully cleaned with distilled water before being rinsed. The cleaned samples were dried in an oven at 75°C to a constant weight. The crop samples were crushed and put through a 0.25 mm sieve for further analysis.

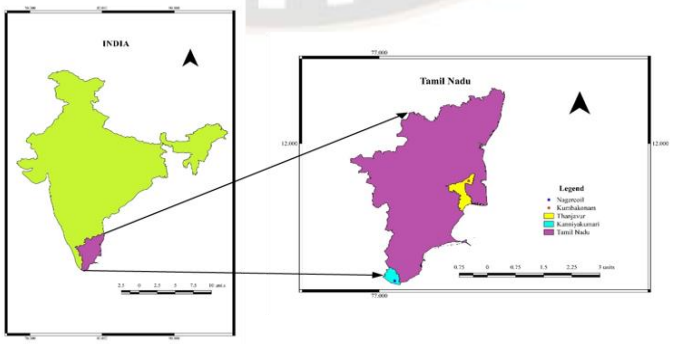

Figure 1: Map showing the Study Area

International Journal on Recent and Innovation Trends in Computing and Communication
ISSN: 2321-8169 Volume: 11 Issue: 9
***Article Received:** 25 July 2023 **Revised:** 12 September 2023 **Accepted:** 30 September 2023*

B. Extraction of Phytoliths

To extract phytoliths from crops, a combination of dry ashing and acid extraction methods was employed. In a muffle furnace, 1 gram of dry plant material was heated to a certain temperature to start the process. The material was subjected to a temperature of 500°C for eight hours. After cooling, the ashed material was transferred to test tubes. To initiate the acid extraction, 20 ml of 10% hydrochloric acid (HCl) was added to the test tubes containing the ashed material. The mixture was then centrifuged at 3500 revolutions per minute (rpm) for 5 minutes, and the resulting supernatant was discarded. Subsequently, this mixture was placed for 20 minutes in a water bath with a temperature of 70 °C. Afterward, the remaining material was rinsed with distilled water, followed by another centrifugation step at 3500 rpm for 5 minutes. Once again, the supernatant was discarded. To continue the extraction process, 20 ml of 15% hydrogen peroxide (H2O2) was added to the test tubes, and for 20 minutes, the mixture was heated in a water bath at 70°C. The supernatant was removed after 5 minutes of centrifugation at 3500 rpm. The remaining material underwent another centrifugation step at 3500 rpm for 5 minutes, followed by washing with distilled water and removal of the supernatant. Finally, to complete the extraction procedure, 1 milliliter of 100% ethanol was added to the test tubes containing the remaining material. The ethanol was allowed to evaporate, leaving behind the extracted phytoliths. This method provides a systematic approach for extracting phytoliths from crops, involving the use of heat, acids, and centrifugation steps to isolate and purify the desired phytolith samples [25].

C. Preparation of slides

In the study conducted by [26], the process of analyzing phytoliths involved several steps. Firstly, the extracted phytoliths were carefully placed on a clean glass slide. To ensure proper visualization, the slide was mounted on Canada balsam, a transparent mounting medium commonly used in microscopy. A needle was then used to mix the phytoliths on the slide, ensuring even distribution across the surface. Afterward, the prepared slide was left to air-dry. To examine the phytoliths, an automated fluorescent microscope called EVOSM 700 was employed. This advanced microscope allows for high-resolution imaging and was set to a magnification of 1000x, enabling detailed observation of the phytoliths. The resulting images were used to analyze and identify the phytoliths based on the International Code for Phytolith Nomenclature 1.0 and 2.0, which provide standardized naming conventions for different types of phytoliths [26][27][28]. This meticulous process ensured the accurate identification and classification of the phytoliths in the study.

D. Extraction of PhytOC

To dissolve the dried, extracted phytolith samples, they were treated with a solution of hydrofluoric acid (HF) at a concentration of 1 mol/L. A temperature of 55°C was used for the entire 60-minute therapy. The organic carbon produced by the dissolved phytoliths after the HF treatment was then dried at 45 °C. To analyze the organic carbon content, a TOC (Total Organic Carbon) analyzer, specifically the SHIMADZU SSM-5000A, was used. This instrument allowed for precise examination and measurement of the organic carbon in the samples [8][29].

E. Data Analysis

In SPSS ("Version 21, SPSS Inc., Wacker Drive, Chicago, USA"), the means were compared using the LSD test to determine the average difference between the contents of phytolith and PhytOC in the rice crop sample data (p b 0.05). In addition, a correlation analysis was performed to investigate the phytolith content of the crop sample, C concentration, and PhytOC. The definitions and the associated formulae are as follows [19]:

F. Phytolith Concentration

Phytoliths are microscopic, silica-based structures that are hard and can be found in various plant tissues. They are formed when plants take up silica from the soil and deposit it within their cells. Phytolith concentration is the number of phytoliths per unit volume of soil. It is expressed as grams per kilogram (g/kg). It is calculated by dividing the weight of the phytoliths in the sample by the weight of the dry plant material.

$$Phytolith\ concentration\ (g/Kg) = \frac{Phytolith\ weight(g)}{Dry\ biomass\ (Kg)} \quad (1)$$

G. Carbon Concentration in Phytolith

Carbon concentration in a phytolith can be defined as the amount of carbon in a phytolith per unit mass of the phytolith. Phytoliths are silica bodies that are formed within plant cells.

$$C\ concentration\ in\ phytolith\ (g/Kg) = \frac{C\ content\ in\ phytolith(g)}{phytolith\ weight\ (Kg)} \quad (2)$$

H. PhytOC concentration

PhytOC concentration is the mass of organic carbon (C) in a phytolith divided by the mass of the phytolith in kilograms. PhytOC stands for phytolith organic carbon. Phytoliths are silica bodies that are formed within plant cells.

International Journal on Recent and Innovation Trends in Computing and Communication
ISSN: 2321-8169 Volume: 11 Issue: 9
***Article Received:** 25 July 2023 **Revised:** 12 September 2023 **Accepted:** 30 September 2023*

Organic carbon is a form of carbon that is found in living and dead organisms.

$$PhytOC\ concentration\ (g/Kg) = \frac{C\ content\ in\ phytolith(g)}{dry\ biomass\ (Kg)} \quad (3)$$

I. PhytOC flux Production

PhytOC flux production is the rate at which phytolith organic carbon (PhytOC) is produced by plants. It is a measure of the amount of organic carbon that is stored in phytoliths. PhytOC flux production (Kg/ha/yr) is the rate at which phytolith organic carbon (PhytOC) is produced by plants per hectare per year.

$$PhytOC\ flux\ Production\ (Kg/ha/yr) = PhytOC\ concentration\ (g/Kg) \times NPP\ (Kg/ha/yr) \times 10^{-3} \quad (4)$$

J. PhytOC production rate

PhytOC production rate is the rate at which phytolith organic carbon (PhytOC) is produced by plants. It is a measure of the amount of organic carbon that is stored in phytoliths per unit time. PhytOC production rate is the amount of PhytOC produced per year in an area. It is measured in kilograms per year (kg/yr).

$$PhytOC\ production\ rate\ (kg/yr) = PhytOC\ production\ flux\ (Kg/ha/yr) \times area\ (ha) \quad (5)$$

4. RESULTS

A. *Results on Phytolith Content*

The phytolith content of the different rice varieties, namely AGB and BGB, exhibited a wide range from 0.9325 to 136.725 g/kg at various stages of growth (Figure 1). In AGB, the highest accumulation of phytoliths occurred during the second stage, while in BGB, the highest levels were observed during the first stage. The phytolith concentration of various rice cultivars is shown in Figure 2 at various growth stages.

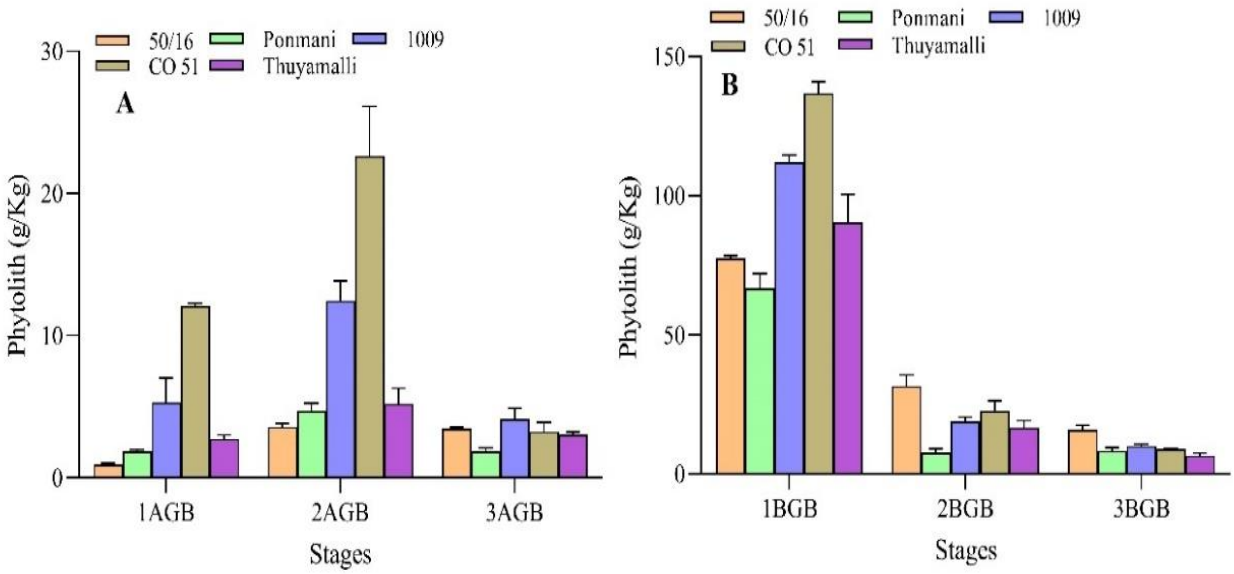

Figure 2: The phytolith content of the rice types AGB (A) and BGB (B) during various growth stages.

The least significant difference (LSD) test indicated significant differences at the P = 0.05 level with various lowercase characters; error bars depict standard error (n = 3).

B. Results on Carbon (C) Content of Phytoliths.

The carbon (C) content of phytoliths showed variations from 0.0086 to 1.4056 g/kg across different growth stages (Figure 2). Generally, in AGB, the C content was highest in the third stage, whereas in BGB, it peaked during the second stage. Figure 3 shows the carbon (C) content of phytoliths.

International Journal on Recent and Innovation Trends in Computing and Communication
ISSN: 2321-8169 Volume: 11 Issue: 9
***Article Received:** 25 July 2023 **Revised:** 12 September 2023 **Accepted:** 30 September 2023*

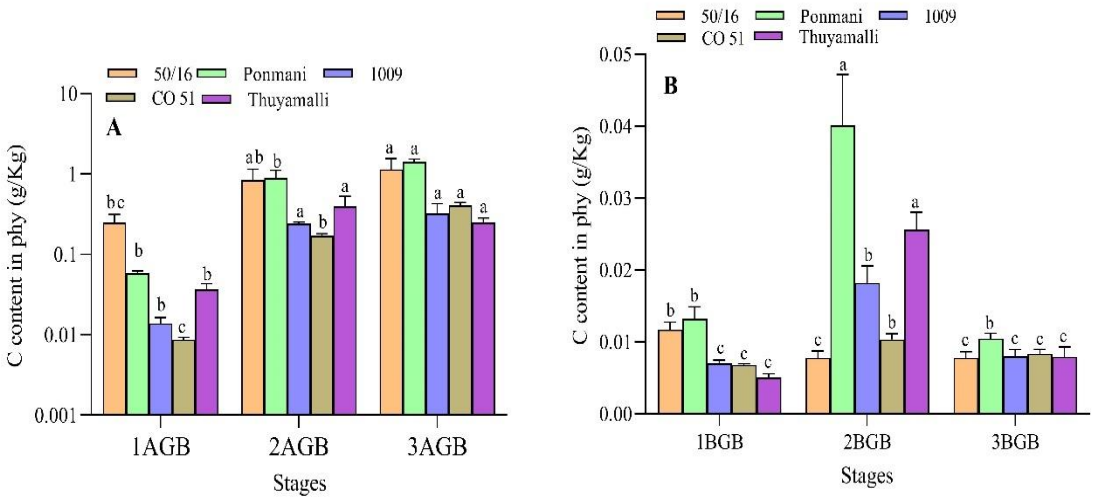

Figure 3: The carbon content of the phytoliths in the rice types AGB (A) and BGB (B) during various stages of growth.

Different lowercase letters exhibit significant differences at the P = 0.05 level, according to the least significant difference (LSD) test; error bars reflect standard error (n = 3).

C. Results on PhytOC Content

The PhytOC content of the different rice varieties ranged from 0.0025 g/kg to 0.07 g/kg (Figure 3). The highest concentrations of PhytOC, measured in terms of dry weight, were found during the second stage in AGB and the first stage in BGB. Figure 4 shows the PhytOC content at different growth stages of rice varieties.

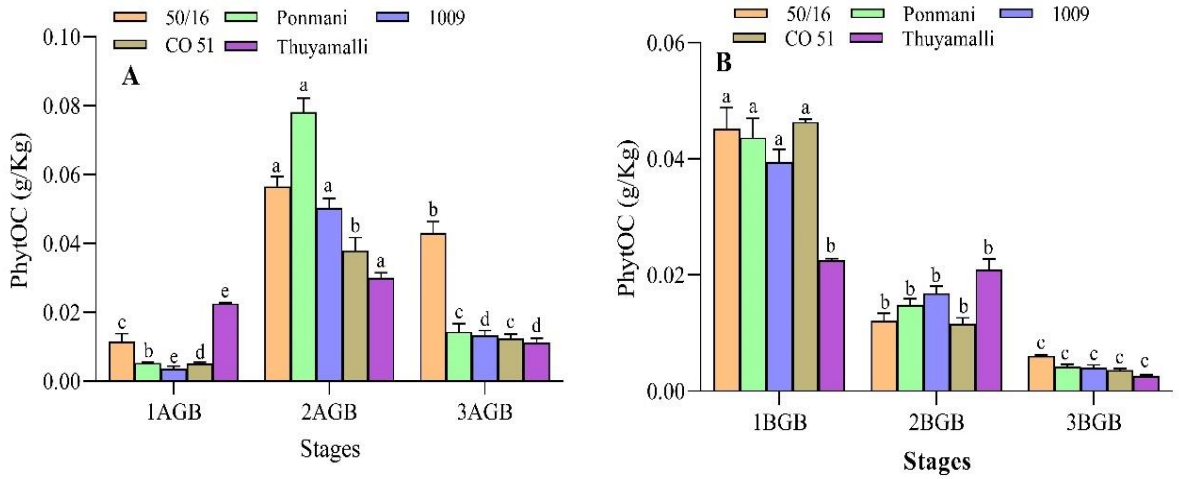

Figure 4: The PhytOC content of the rice types AGB (A) and BGB (B) during various growth stages.

Different lowercase letters indicate significant differences at the P = 0.05 level, according to the least significant difference (LSD) test; error bars show standard error (n = 3).

D. Results on PhytOC Flux Production Rate

The annual production of PhytOC by the plant is measured by PhytOC production flux. PhytOC flux production rate refers to the rate at which carbon is sequestered into phytoliths. Understanding the PhytOC flux production

International Journal on Recent and Innovation Trends in Computing and Communication
ISSN: 2321-8169 Volume: 11 Issue: 9
***Article Received:** 25 July 2023 **Revised:** 12 September 2023 **Accepted:** 30 September 2023*

rate is important for understanding the potential of phytoliths as a tool for carbon sequestration and climate change mitigation. Therefore, the study revealed that ranging from 0.124 to 0.8361 Kg/ha/yr in the 1st and 2nd stages ponmani produces more PhytOC than the other rice varieties, and in 3rd stage 50/16. Figure 5 estimated the PhytOC Production Flux and rate of Rice varieties at different growth stages.

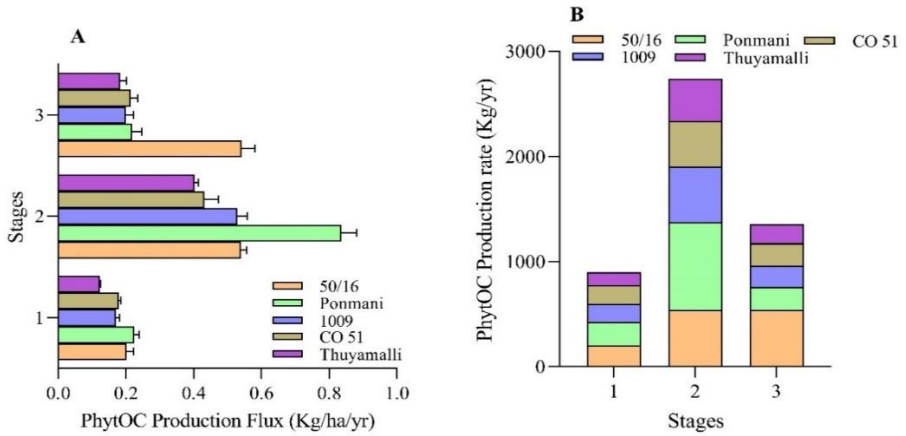

Figure 5: Estimation of PhytOC Production Flux (A) and rate (B) of Rice varieties at different growth stages.

Note: error bars represent standard errors. (n = 3)

E. Results on PhytOC Production Rate

PhytOC production rate is the total PhytOC production of an area ranging from 899.64 to 1375.09 Kg/yr in the 1st and 2nd stages ponmani produces more PHTYOC than the other rice varieties and in 3rd stage 50/16. Combining AGB and BGB. The carbon occlusion in phytolith per year for a hectare of rice can be 1375.09 Kg/yr. Therefore, upon the crop's demise, when released into the soil, the PhytOC present in these crops' aids in long-term terrestrial carbon sequestration.

F. Distribution of phytolith

The distribution of phytoliths refers to their occurrence and abundance in various parts of plants. Phytoliths are microscopic silica structures that can be found in different tissues, including leaves, stems, roots, and reproductive organs. Their distribution provides insights into the deposition patterns and accumulation rates of phytoliths within different plant species and varieties. Phytoliths can exhibit diverse morphotypes such as bilobate, elongate, lanceolate, cross, trapeziform, rectangular, and more. Throughout the growth of the rice crop varieties in AGB, the dominant morphotypes were bilobates, elongated, bulliform, and rectangular, while in BGB, polyhedral morphotypes prevailed (Table 1). Acicular morphotype and husk phytoliths were only observed during the third stage of crop growth. Understanding the distribution of phytoliths is valuable for studying plant evolution, ecological interactions, and environmental adaptations.

G. Distribution of phytolith in AGB of Rice Variety

The distribution of phytoliths in the above-ground parts (AGB) of rice focuses on understanding the pattern and abundance of phytoliths in the aerial parts of the rice plants. The analysis reveals a diverse distribution of phytoliths within the AGB, including different morphotypes such as bilobate, elongate, lanceolate, cross, trapeziform, rectangular, and more. This distribution provides insights into the deposition and growth of phytoliths in various parts of the rice plants, contributing to our understanding of their role in plant physiology, growth, and environmental adaptation.

TABLE 1: Distribution of various phytolith in AGB of Rice varieties at different Growth stages

Crop Variety	**Age**	**Phytolith Morphotypes**
Ponmani	1AGB	Bilobate; Elongate

International Journal on Recent and Innovation Trends in Computing and Communication
ISSN: 2321-8169 Volume: 11 Issue: 9
***Article Received:** 25 July 2023 **Revised:** 12 September 2023 **Accepted:** 30 September 2023*

	2AGB	Arcuate scrobiculate; Bilobate; Rectangular crenate; Rectangular nodulate; Cross; Rectangular Gibbate; Rectangular papillar; Amoeboid; Geniculate; Rugulate
	3AGB	Rectangular; Rectangular gibbate; Elongate psilate; Elongate crenate; Rectangular psilate; Elongate echinate
50/16	1AGB	Bilobate; Cross; Spheroidal; Bulliform Epidermal sheet
	2AGB	Acicular aerolate; Bulliform; Cross; Bilobate; Papillar; Tuberculate; Bulliform Epidermal sheet
	3AGB	Bilobate; Cross; Polyhedral; Elongated crenate; amoeboid; Elongated echinate; Elongated Papillate; Elongated Gibbate; Ovate; Elongated aerolate; Elongated Scrabiculate; Carinate; Trapiziform Sinuate; Elongate; Acicular; Arcurate
1009	1AGB	Arcuate; Epidermal flat sheet; Bulliform; Elongated crenate; Bilobate; Elongated echinate; Spheroidal;
	2AGB	Saddle; Elongate; Hair base; Elongate Papillar; Elongate Baculate; Bilobate; Elongate Scrabiculate; Vessel and bundle sheath cell; Elongated Gibbate
	3AGB	Bilobate; Arcuate; Elongate Gibbate; Rectangular Striate; Vessel and bundle sheath cell; Ovate; Flabellate; Amoeboid; Elongate; Parallepipedal bulliform dentate; Elongate echinate; Acicular; Clavate; Elongate Echinate
CO 51	1AGB	Bilobate; Elongated with bilobate; Elongate Sinuate; Flabellate; Oblong
	2AGB	Arcuate; Elongate Columellate; Elongate Gibbate; Bilobate; Parallepipedal bulliform; Elongate Echinate; Elongate Verucate; Elongate Scrabiculate; Flabellate; Acicular; Amoeboid; Arcuate; Globular Granulate; Cylindrical; Elongate Sinuate; Oblong
	3AGB	Bilobate; Elongate Papillate; Vessel and bundle sheath cell; Elongate Gibbate; Elongate with Ovate; Elongated crenate; Oblong Crenate; Elongate Dentate; Elongate Tuberculate; Elongate Echinate; Flabellate; Cross; Acicular
Thuyamalli	1AGB	Bilobate; Elongate Papillate; Elongate Echinate; Rectangular; Elongate Psilate; Elongate Crenate; Cross; Cylindrical; Circular; Ovate
	2AGB	Bilobate; Elongate Baculate; Cross with Elongate; Elongate Psilate; Elongate Papillate; Cross; Elongate Dentate; Elongate Sinuate; Parallepipedal bulliform; Ciricular; Elongate Scrabiculate
	3AGB	Bilobate; Elongate Castellate; Elongate with Ovate; Spheroidal; Parallepipedal bulliform; Elongate Baculate; Flabellate; Cylindrical; Elongate Tuberculate; Elongate Pilate; Acicular; Rectangular; Elongate Sinuate; Elongate Dentate; Spheroidal Psilate

Table 1 describes that the Crop variety "Ponmani" displays bilobate and elongated phytolith morphotypes at 1AGB. At 2AGB, it develops additional morphotypes including arcuate scrobiculate, rectangular crenate, cross, and amoeboid. By 3AGB, it exhibits elongate psilate and rectangular gibbate morphotypes. The crop variety "50/16" at 1AGB has bilobate and spheroidal morphotypes, while at 2AGB, it shows acicular aerolate, papillar, and tuberculate morphotypes. At 3AGB, it includes elongated crenate and amoeboid morphotypes. Crop variety "1009" presents arcuate, bulliform, and elongated crenate morphotypes at 1AGB. At 2AGB, saddle and vessel and bundle sheath cell morphotypes emerge, while at 3AGB, elongate gibbate and flabellate morphotypes are observed. Crop variety "CO 51" exhibits elongate sinuate and elongate gibbate morphotypes at 1AGB, elongate columellate and acicular morphotypes at 2AGB, and elongate papillate and oblong morphotypes at 3AGB.

H. Distribution of phytolith in BGB of Rice Variety

The distribution of phytoliths in the below-ground parts (BGB) of rice examines the presence and abundance of phytoliths in the roots and other below-ground structures of rice plants. The analysis reveals a varied distribution of phytoliths within the BGB, encompassing different morphotypes such as elongate, tuberculate, polyhedral, and more. This distribution provides valuable insights into the deposition and accumulation patterns of phytoliths in the underground parts of rice plants, shedding light on their potential functions in root development, nutrient uptake, and plant-soil interactions.

International Journal on Recent and Innovation Trends in Computing and Communication
ISSN: 2321-8169 Volume: 11 Issue: 9
***Article Received:** 25 July 2023 **Revised:** 12 September 2023 **Accepted:** 30 September 2023*

TABLE 2: Distribution of various phytolith in BGB of rice varieties at different growth stages

Crop Variety	Age	Phytolith Morphotypes
Ponmani	1BGB	Acicular Crenate; Bilobate; Lanceolate; Cross; Trapeziform; Rectanglular; Polyhedral
	2BGB	Arcuate crenate; Bilobate epidermis sheet; Reniform; Oblong; Elongate; Tuberculate; Circular
	3BGB	Polygonal
50/16	1BGB	Elongate; Bilobate; Polyhedral
	2BGB	Ovate granulate; Orbicular; Bulliform epidermal Sheet; Rectangular; Polyhedral
	3BGB	Bilobate; Cross; Polyhedral; Elongated crenate
1009	1BGB	Elongated Psilate; Elongate; Polyhedral
	2BGB	Elongate Crenate; Cylindrical; Arcuate dentate; Epidermal flat sheet; Elongate with cross
	3BGB	Polyhedral
CO 51	1BGB	Bilobate; Elongated; Polyhedral
	2BGB	Elongate crenate; Parallepipedal bulliform; saddle with the sheet; polyhedral
	3BGB	Bilobate; Polyhedral; Ellipsoidal; Acicular
Thuyamalli	1BGB	Bilobate; Polyhedral; Rectangular
	2BGB	Bilobate; Polyhedral; Parallepipedal bulliform; Elongate gibbate
	3BGB	Bilobate; polyhedral

Table 2 depicts that the crop variety "Ponmani" at 1BGB displays various phytolith morphotypes, including acicular crenate, bilobate, lanceolate, cross, trapeziform, rectangular, and polyhedral. At 2BGB, it exhibits arcuate crenate, bilobate epidermis sheet, reniform, oblong, elongate, tuberculate, and circular morphotypes. As it reaches 3BGB, polygonal morphotypes are observed. "50/16" at 1BGB shows elongate, bilobate, and polyhedral morphotypes, while at 2BGB, ovate granulate, orbicular, bulliform epidermal sheet, rectangular, and polyhedral morphotypes are present. At 3BGB, it includes bilobate, cross, polyhedral, and elongated crenate morphotypes. "1009" exhibits elongated psilate, elongate, and polyhedral morphotypes at 1BGB, while at 2BGB, it shows elongate crenate, cylindrical, arcuate dentate, epidermal flat sheet, and elongate with cross morphotypes. At 3BGB, polyhedral morphotypes are observed. "CO 51" displays bilobate, elongated, and polyhedral morphotypes at 1BGB, elongate crenate, parallelepipedal bulliform, saddle with a sheet, and polyhedral morphotypes at 2BGB, and bilobate, polyhedral, ellipsoidal, and acicular morphotypes at 3BGB. "Thuyamalli" exhibits bilobate, polyhedral, and rectangular morphotypes at 1BGB, bilobate, polyhedral, parallelepipedal bulliform, and elongate gibbate morphotypes at 2BGB, and bilobate and polyhedral morphotypes at 3BGB.

I. Matrix on Pearson Correlations

The Pearson correlations matrix explores the relationships between phytolith, PhytOC, and C (carbon) within the phytoliths of AGB and BGB at different growth stages. This analysis provides insights into the associations between these variables. By examining the correlations, we can better understand the interplay between phytolith content, PhytOC, and carbon within the phytoliths as the plants progress through different growth stages. There was generally no correlation between phytolith and PhytOC contents during different growth stages, except in the third stage of BGB where a strong positive correlation was observed ($R2 = 0.944$, $p < 0.05$) (Figure 4). However, a significant negative correlation was noted between phytoliths and C during the second stage for both AGB ($R2 = -0.880$, $p < 0.05$) and BGB ($R2 = -0.911$, $p < 0.05$). Furthermore, a strong positive correlation was found between PhytOC and C during the first stage of AGB ($R2 = 0.987$, $p < 0.05$). Figure 6 gives the Pearson correlations matrix between Phytolith, PhytOC, and C within phytolith AGB and BGB.

International Journal on Recent and Innovation Trends in Computing and Communication
ISSN: 2321-8169 Volume: 11 Issue: 9
Article Received: *25 July 2023* ***Revised:*** *12 September 2023* ***Accepted:*** *30 September 2023*

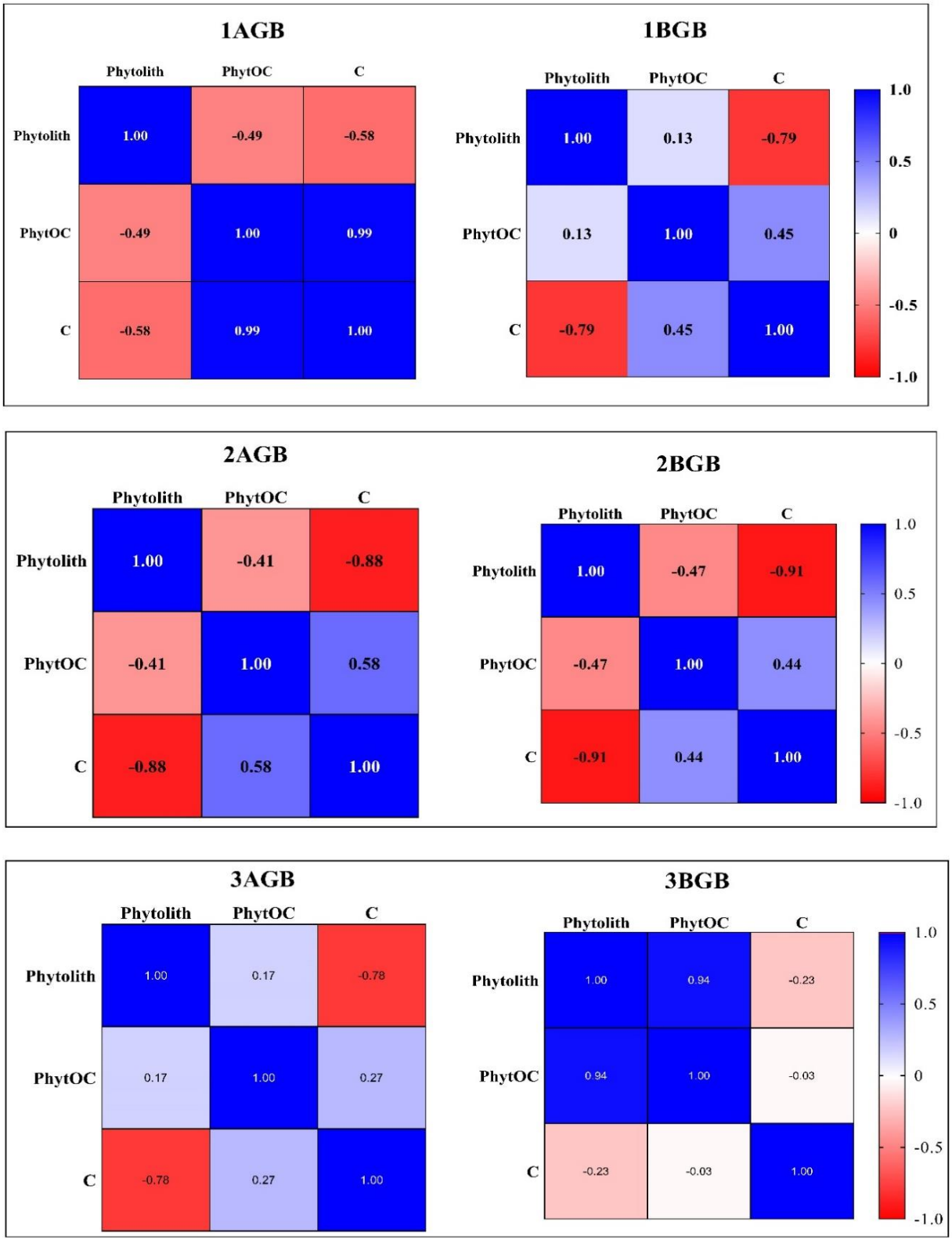

Figure 6: Pearson correlations matrix between Phytolith, PhytOC, and C within phytolith AGB and BGB at different growth stages (significant correlation $p < 0.005$).

International Journal on Recent and Innovation Trends in Computing and Communication
ISSN: 2321-8169 Volume: 11 Issue: 9
***Article Received:** 25 July 2023 **Revised:** 12 September 2023 **Accepted:** 30 September 2023*

J. Phytolith Morphotypes Images on different rice varieties

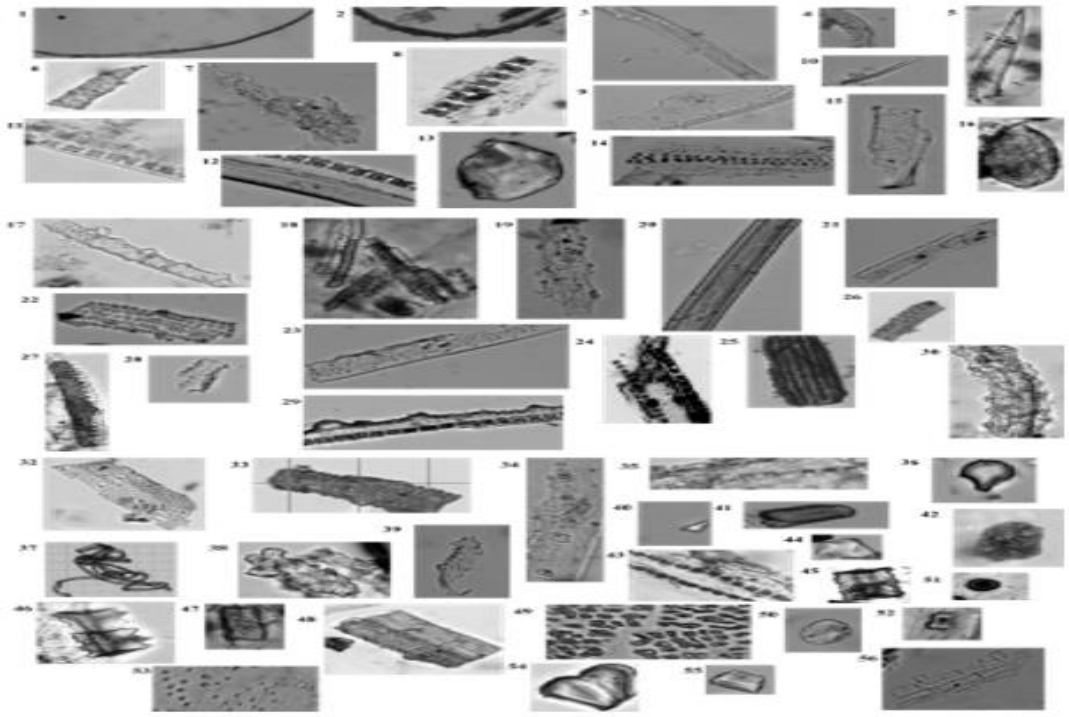

Figure 7: Phytolith Morphotypes of different rice varieties: 1 Arcuate, 2 Arcuate Dentate, 3 Arcuate Scrobiculate, Arcuate Crenate, 5 Acicular, 6 Acicular Aerolate, 7 Amoeboid, 8 Bilobate, 9 Bilobate epidermis sheet, 10 Cylindrical, 11 Cross, 12 Cross with elongate, 13 circular, 14 Elongate with bilobate, 15 epidermis Flat sheet phytolith, 16 ellipsoidal, 17 Elongate crenate, 18 Elongate echinate, 19 Elongate papillate 20 Elongate psilate, 21 Elongate Baculate, 22 Elongate gibbate, 23 Elongate scrabiculate, 24 Elongate dentate, 25 Elongate sinuate, 26 Elongate castellate, 27 Elongate pilate, 28 Elongate columellate, 29 Elongate verucate, 30 Elongate aerolate, 31 Elongate tuberculate, 32 Elongate papillar, 33 Elongate nodulate, 34 Elongate with cross, 35 Elongate with ovate, 36 flabellate, 37 geniculate, 38 husk phytolith, 39 hair base, 40 lanceolate, 41 oblong, 42 ovate granulate, 43 orbicular, 44 polyhedral, 45 parallepipedal bulliform, 46 parallepipedal bulliform detate, 47 rectangular, 48 rectangular striate, 49 reniform, 50 spheroidal, 51 spheroidal psilate, 52 saddle, 53 saddle with sheet, 54 trapiziform sinuate, 55 trapiziform, 56 Vessel and Bundle Sheath Cell.

5. DISCUSSIONS

A. Phytolith and its Morphotypes in AGB and BGB

The phytolith content was found to be consistently higher in Below-Ground Biomass (BGB) compared to Above-Ground Biomass (AGB) across all growth stages in various rice varieties. Among the AGB samples, the rice variety CO51 exhibited the highest phytolith content, with values of 12.07 g/kg in the first growth stage (1AGB) and 22.34 g/kg in the second growth stage (2AGB). Another variety, 1009, had a phytolith content of 4.11 g/kg in the third growth stage (3AGB), while the lowest values were observed in the 50/16 variety (1AGB: 0.93 g/kg; 2AGB: 3.56 g/kg) and Ponmani (3AGB: 1.82 g/kg). In contrast, within the BGB samples, CO51 displayed the highest phytolith content (1BGB: 136.7 g/kg), followed by 50/16 (2BGB: 31.53 g/kg; 3BGB: 15.7 g/kg), while the lowest values were recorded in Ponmani (1BGB: 66.62 g/kg; 2BGB: 7.5 g/kg) and Thuyamalli (3BGB: 6.49 g/kg). These findings are consistent with previous studies conducted on plant species from the Poaceae family, such as bamboo, buckwheat, grasses from grasslands, and steppes [30][31][32]. Rice crops belong to the monocot group, which exhibits a significantly higher accumulation of phytolith content in their living tissue compared to dicot plants due to differences in their root structures, as described in previous studies [5].

This study provides evidence that the maturity of the plant plays a role in phytolith formation in crops. Phytolith accumulation is a gradual process that occurs throughout the plant's life cycle, and therefore, phytolith formation generally increases with plant age [33].

International Journal on Recent and Innovation Trends in Computing and Communication
ISSN: 2321-8169 Volume: 11 Issue: 9
***Article Received:** 25 July 2023 **Revised:** 12 September 2023 **Accepted:** 30 September 2023*

The current investigation examined the phytolith morphotypes (microscopic silica structures) produced by different varieties of rice at various stages of growth. The study found that each rice variety exhibited a diverse range of phytolith types during different phases of growth. The number of distinct phytolith shapes increased as the rice crops matured, with the variety BGB displaying fewer shapes than AGB in the later stages. During the initial stage, BGB showcased a high degree of phytolith shape diversity. The prominent types of phytoliths observed in BGB included polyhedral, elongated, and AGB shapes. Notably, the varieties Thuyamalli (AGB) and 50/16 (BGB) accumulated a wide variety of phytolith shapes, while Ponmani (AGB) and 1009 (BGB) exhibited the lowest diversity in this stage. Moving to the second stage, AGB demonstrated a greater array of phytolith types compared to BGB. Ponmani and CO51 (AGB) as well as Ponmani and 50/16 (BGB) displayed a high abundance of phytolith types, whereas 1009 and Thuyamalli (AGB) and 1009, CO51, and Thuyamalli (BGB) had the lowest diversity. In the third stage, the phytolith types in BGB notably decreased compared to the earlier growth stages. The study observed a significant reduction in phytolith morphotypes as the crops aged. Among the varieties, 1009 (AGB) and 50/16 (BGB) exhibited a high abundance of phytolith types, while Ponmani (AGB) and Ponmani and 1009 (BGB) had the lowest diversity.

The most common phytolith shapes observed were elongated, bilobates, rectangular, and bulliform. Interestingly, the acicular shape was exclusively found in the seed stalk of all rice varieties and only on the 120th day of growth. These findings align with previous studies, including the works of [33][34], which also reported changes in phytolith assemblages throughout the rice growing season and their correlation with the age and maturity of the crops. The study on crop varieties revealed a distinct pattern in terms of their growth stages and the presence of phytoliths, which are microscopic silica structures found in plant tissues. During the first stage, the crop known as BGB exhibited higher levels of PhytOC and aboveground biomass (AGB) compared to the second and third stages. Among the AGB crops, Thuyamalli displayed the highest phytolith content, with values of 0.022 g/Kg in the first stage, 0.07 g/Kg in the second stage (Ponmani), and 0.042 g/Kg in the third stage (50/16). On the other hand, the lowest phytolith content was observed in 1009 (0.003 g/Kg) in the first stage, Thuyamalli (0.029 g/Kg) in the second stage, and Thuyamalli (0.011 g/Kg) in the third stage. Regarding belowground biomass (BGB), CO51 exhibited the highest phytolith content at 0.046 g/Kg in the first stage, followed by Thuyamalli (0.020 g/Kg) in the second stage, and 50/16 (0.006 g/Kg) in the third stage. Conversely, the lowest phytolith content was found in Thuyamalli (0.022 g/Kg) in the first stage, CO51 (0.011 g/Kg) in the second stage, and Thuyamalli (0.002 g/Kg) in the third stage.

Recent investigations have shown the crucial part that BGB plays in the sequestration of PhytOC in various ecosystems such as bamboo forests, grasslands, and steppes [29][30]. However, in this particular study, the highest PhytOC content was only observed during the first stage, potentially due to the early growth phase of the crop. As the crop biomass increased in AGB, there was a corresponding increase in the PhytOC content. To enhance PhytOC production in crop tissues and achieve the maximum PhytOC sequestration potential, intensive management practices like fertilization and tillage can be employed [35]. These measures promote the accumulation of PhytOC and contribute to carbon sequestration in agricultural systems.

The findings of the study revealed various relationships between phytolith and PhytOC in different growth stages of the plant. Moderate negative relationships were observed in 1AGB, 2AGB, and 2BGB, indicating that as the phytolith increased, PhytOC decreased. Conversely, weak and strong positive correlations were found in 1BGB, 3AGB, and 3BGB, suggesting that higher phytolith deposition was associated with higher PhytOC content. These results suggest that the relative yields of PhytOC are influenced by both phytolith deposition and the effectiveness of C trapping inside phytoliths as opposed to the amount of phytoliths absorbed by plants. Previous studies by [36-37][16] support these findings. Furthermore, the relationship between phytolith and carbon (C) content displayed a strong negative correlation across all growth stages. This implies that the effectiveness of C occlusion in phytoliths when plants are growing affects the carbon sequestration potential. This finding is consistent with the study conducted by [36]. Notably, the correlation between PhytOC and C content within phytoliths highlights the significant role of phytoliths as a tool for carbon sequestration. Several studies, such as those by [9][38][28][22], have also indicated a positive correlation, emphasizing the importance of phytoliths in carbon sequestration. In this study, the results align with previous research, demonstrating a strong positive correlation between PhytOC and C content within phytoliths in 1AGB and 2AGB. Moderate positive relationships were observed in 1BGB and 2BGB, while weak positive and weak negative correlations were found in 3AGB and 3BGB, respectively. These findings suggest that as the crop ages, the efficiency of C sequestration within phytoliths decreases, with the third growth stage exhibiting lower efficiency. It is noteworthy that AGB displayed higher efficiency of phytolith carbon sequestration compared to BGB. Overall, this study sheds light on the relationships between phytolith, PhytOC, and carbon content within phytoliths at different growth stages of the crop. The results emphasize the influence of phytolith

deposition and the effectiveness of C capturing in phytoliths on the relative yields of PhytOC. Furthermore, the study underscores the potential significance of phytoliths as a tool for carbon sequestration, with varying efficiency observed in different growth stages. These findings contribute to our understanding of carbon sequestration processes and emphasis the significance of taking phytoliths into consideration as a carbon sink in agricultural systems.

6. CONCLUSIONS

This research looked into the impact of crop growing stage on the formation and ability of carbon occlusion within phytoliths in rice varieties. The findings revealed significant variations in the formation and carbon occlusion capacity of phytoliths at different growth stages. As the rice plants progressed through growth stages, there were notable changes in the quantity and quality of carbon occlusion within the phytoliths. This indicates that the growth stage plays a crucial role in shaping the carbon occlusion process in phytoliths. Understanding these dynamics is essential for comprehending the C sequestration potential of rice crops and developing strategies to enhance carbon storage in agricultural systems. Further research is warranted to explore the underlying mechanisms driving these stage-dependent changes in phytolith formation and carbon occlusion in rice varieties.

REFERENCES

[1] Singh, M.K. and Prasad, S.K., 2014. Agronomic aspects of zinc biofortification in rice (Oryza sativa L.). Proceedings of the national academy of Sciences, India Section B: Biological Sciences, 84, pp.613-623.

[2] Prasad, R., Shivay, Y.S. and Kumar, D., 2017. Current status, challenges, and opportunities in rice production. Rice production worldwide, pp.1-32.

[3] Yoro, K.O. and Daramola, M.O., 2020. CO2 emission sources, greenhouse gases, and the global warming effect. In Advances in carbon capture (pp. 3-28). Woodhead Publishing.

[4] Mangalassery, S., Sjögersten, S., Sparkes, D.L., Sturrock, C.J., Craigon, J. and Mooney, S.J., 2014. To what extent can zero tillage lead to a reduction in greenhouse gas emissions from temperate soils? Scientific reports, 4(1), pp.1-8.

[5] Nawaz, M.A., Zakharenko, A.M., Zemchenko, I.V., Haider, M.S., Ali, M.A., Imtiaz, M., Chung, G., Tsatsakis, A., Sun, S. and Golokhvast, K.S., 2019. Phytolith formation in plants: from soil to cell. Plants, 8(8), p.249.

[6] Tripathi, D.K., Vishwakarma, K., Singh, V.P., Prakash, V., Sharma, S., Muneer, S., Nikolic, M., Deshmukh, R., Vaculik, M. and Corpas, F.J., 2021. Silicon crosstalk with reactive oxygen species, phytohormones, and other signaling molecules. Journal of Hazardous Materials, 408, p.124820.

[7] Katz, O., 2019. Silicon content is a plant functional trait: implications in a changing world. Flora, 254, pp.88-94.

[8] Li, Z., Song, Z., Parr, J.F. and Wang, H., 2013. Occluded C in rice phytoliths: implications to biogeochemical carbon sequestration. Plant and soil, 370, pp.615-623.

[9] Song, A., Ning, D., Fan, F., Li, Z., Provance-Bowley, M. and Liang, Y., 2015. The potential for carbon bio-sequestration in China's paddy rice (Oryza sativa L.) as impacted by slag-based silicate fertilizer. Scientific reports, 5(1), pp.1-12.

[10] Kundu, S., Rajendiran, S., Vassanda Coumar, M. and Ajay, 2020. Effect of land use and management practices on quantifying changes of phytolith-occluded carbon in arable soils. Carbon Management in Tropical and Sub-Tropical Terrestrial Systems, pp.37-55.

[11] Biswal, A.K. and Kohli, A., 2013. Cereal flag leaf adaptations for grain yield under drought: knowledge status and gaps. Molecular Breeding, 31, pp.749-766.

[12] Reddy, K.R., Seghal, A., Jumaa, S., Bheemanahalli, R., Kakar, N., Redoña, E.D., Wijewardana, C., Alsajri, F.A., Chastain, D., Gao, W. and Taduri, S., 2021. Morpho-physiological characterization of diverse rice genotypes for seedling stage high-and low-temperature tolerance. Agronomy, 11(1), p.112.

[13] Mueller, B.S.D.F., Sakamoto, T., Silveira, R.D.D., Zambussi-Carvalho, P.F., Pereira, M., Pappas, G.J., do Carmo Costa, M.M., Guimarães, C.M., Pereira, W.J., Brondani, C. and Vianello-Brondani, R.P., 2014. Differentially expressed genes during flowering and grain filling in common bean (Phaseolus vulgaris) grown under drought stress conditions. Plant molecular biology reporter, 32, pp.438-451.

[14] Parr, J.F. and Sullivan, L.A., 2014. Comparison of two methods for the isolation of phytolith occluded carbon from plant material. Plant and soil, 374, pp.45-53.

[15] Debnath, N., Nath, A., Sileshi, G.W., Nath, A.J., Nandy, S. and Das, A.K., 2023. Determinants of phytolith occluded carbon in bamboo stands across forest types in the eastern Indian Himalayas. Science of The Total Environment, 857, p.159568.

[16] Sun, X., Liu, Q., Gu, J., Chen, X. and Zhu, K., 2016. Evaluation of the occluded carbon within husk phytoliths of 35 rice cultivars. Frontiers of Earth Science, 10, pp.683-690.

[17] Zuo, X., Lu, H. and Gu, Z., 2014. Distribution of soil phytolith-occluded carbon in the Chinese Loess Plateau

and its implications for silica–carbon cycles. Plant and soil, 374, pp.223-232.

[18] Ru, N., Yang, X., Song, Z., Liu, H., Hao, Q., Liu, X. and Wu, X., 2018. Phytoliths and phytolith carbon occlusion in aboveground vegetation of sandy grasslands in eastern Inner Mongolia, China. Science of the Total Environment, 625, pp.1283-1289.

[19] Yang, X., Song, Z., Liu, H., Bolan, N.S., Wang, H. and Li, Z., 2015. Plant silicon content in forests of north China and its implications for phytolith carbon sequestration. Ecological Research, 30, pp.347-355.

[20] Yang, X., Song, Z., Qin, Z., Wu, L., Yin, L., Van Zwieten, L., Song, A., Ran, X., Yu, C. and Wang, H., 2020. Phytolith-rich straw application and groundwater table management over 36 years affect the soil-plant silicon cycle of a paddy field. Plant and Soil, 454, pp.343-358.

[21] Si, Y., Wang, L., Zhou, Q., and Huang, X., 2018. Effects of lanthanum and silicon stress on bio-sequestration of lanthanum in phytoliths in rice seedlings. Environmental Science and Pollution Research, 25, pp.10752-10770.

[22] Anjum, M. and Nagabovanalli, P.B., 2021. Assessing production of phytolith and phytolith occluded carbon in above-ground biomass of intensively cultivated rice ecosystems in India. Carbon Management, 12(5), pp.509-519.

[23] Wang, X., Qi, J.Y., Zhang, X.Z., Li, S.S., Virk, A.L., Zhao, X., Xiao, X.P. and Zhang, H.L., 2019. Effects of tillage and residue management on soil aggregates and associated carbon storage in a double paddy cropping system. Soil and Tillage Research, 194, p.104339.

[24] Weisskopf, A., Harvey, E., Kingwell-Banham, E., Kajale, M., Mohanty, R. and Fuller, D.Q., 2014. Archaeobotanical implications of phytolith assemblages from cultivated rice systems, wild rice stands, and macro-regional patterns. Journal of Archaeological Science, 51, pp.43-53.

[25] Rajendiran, S., Coumar, V., Dotaniya, M. L., & Kumar, A. (2016). Carbon occlusion potential of rice phytoliths: implications for global carbon cycle and climate change mitigation. Appl Ecol Environ Res, 14(2), 265-281.

[26] Zhan, H., Juan, L., Zhao-Hui, N., Li, M. B., Wang, C. M., & Wang, S. G. (2019). Silicon variation and phytolith morphology in different organs of Dendrocalamus brandisii (Munro) Kurz (Bambusoideae). Brazilian Journal of Botany, 42(3), 529-541.

[27] Madella, M., Alexandre, A., & Ball, T. (2005). International code for phytolith nomenclature 1.0. Annals of botany, 96(2), 253-260.

[28] David, R., Byrt, C.S., Tyerman, S.D., Gilliham, M., & Wege, S. (2019). International Code for Phytolith Nomenclature 2.0 (ICPN 2.0). Annals of Botany, 124(2), 209-220.

[29] Sun, X., Liu, Q., Tang, T., Chen, X., & Luo, X. (2019). Silicon fertilizer application promotes phytolith accumulation in rice plants. Frontiers in plant science, 10, 425.

[30] Chen, C., Huang, Z., Jiang, P., Chen, J., & Wu, J. (2018). Belowground phytolith-occluded carbon of monopodial bamboo in China: An overlooked carbon stock. Frontiers in Plant Science, 9, 1615.

[31] Qi, L., Sun, T., Guo, X., Guo, Y., & Li, F.Y. (2021). Phytolith-occluded carbon sequestration potential in three major steppe types along a precipitation gradient in Northern China. Ecology and Evolution, 11(3), 1446–1456. https://doi.org/10.1002/ece3.7155

[32] Wang, L., & Sheng, M. (2022). Phytolith occluded organic carbon in Fagopyrum (Polygonaceae) plants: Insights on the carbon sink potential of cultivated buckwheat planting. Frontiers in Plant Science, 13. https://doi.org/10.3389/fpls.2022.1014980

[33] Li, R., Fan, J., Carter, J., Jiang, N., & Gu, Y. (2017). Monthly variations of phytoliths in the leaves of the bamboo Dendrocalamus ronganensis (Poaceae: Bambusoideae). Review of Palaeobotany and Palynology, 246, 62-69.

[34] Li, R., Chen, X., Wen, M., Vachula, R.S., Tan, S., Dong, H., ... & Xu, M. (2022). Phytolith-occluded carbon in leaves of Dendrocalamus Ronganensis influenced by drought during the growing season. Physiologia Plantarum, 174(5), e13748.

[35] Huang, C., Li, Y., Wu, J., Huang, Z., Chang, S.X., & Jiang, P. (2019). Intensive management increases phytolith-occluded carbon sequestration in Moso bamboo plantations in subtropical China. Forests, 10(10), 883.

[36] Parr, J.F., & Sullivan, L.A. (2011). Phytolith occluded carbon and silica variability in wheat cultivars. Plant and Soil, 342(1), 165-171.

[37] Sun, X., Liu, Q., Zhao, G., Chen, X., Tang, T., & Xiang, Y. (2017). Comparison of phytolith-occluded carbon in 51 main cultivated rice (Oryzasativa) cultivars of China. RSC advances, 7(86), 54726-54733.

[38] Prajapati, K., Rajendiran, S., Coumar, M. V., Dotaniya, M. L., Kumar, A., & Kundu, S. (2016). Carbon occlusion potential of rice phytoliths: implications for global carbon cycle and climate change mitigation. Appl Ecol Environ Res, 14(2), 265-281.